

Self-Quenching Effect of the Decay of Localized Surface Plasmons: Classical and Quantum Perspectives

Krystyna Kolwas

Institute of Physics, Polish Academy of Sciences, Aleja Lotników 32/46,
02-668 Warsaw, Poland.

Contributing authors: Krystyna.Kolwas@ifpan.edu.pl;

Abstract

This study presents a self-consistent, quantum-informed model for the decay dynamics of localized surface plasmons (LSPs) in spherical metal nanoparticles (NPs), described as plasmonic quasi-particles (PQPs). By bridging classical electrodynamics description for quasi-normal modes (retardation effects included) with a quantum emitter perspective, this framework provides an analytically tractable description of the damping of the dissipative confined plasmonic systems. In addition to its significance for emission control, the model emphasizes the bosonic characteristics of plasmonic quasi-particles, which are coherent many-electron excitations of the states of quasi-normal modes. Unlike conventional cavity quantum electrodynamics (CQED), where the emitter and cavity exist as separate systems, a plasmonic quasi-particle functions as a quantum emitter embedded within a self-created resonant near-field nano-cavity of confined radial fields, sharing the spectral characteristics of the surface transverse-magnetic (TM) modes, which include nonradiative damping effects resulting from, e.g., ohmic losses in a metal. This work extends Fermi's Golden Rule to include the coupling between the emission process and the self-generated cavity impact. The derived self-consistent formulation offers analytical expressions for the total damping rates, which demonstrate a size-dependent suppression displayed in higher multipolarity modes attributed to the impact of the self-quenching effect resulting from the coaction of radiative and non-radiative channels.

Keywords: Localized Surface Plasmons, decay dynamics, spontaneous emission, quasi-particles, dispersion relation, cavity electrodynamics, Fermi's Golden Rule, self-quenching

1 Introduction

Nanometallic (plasmonic) structures exhibit a remarkable ability to confine and concentrate electromagnetic (EM) field energy within subwavelength volumes, making them essential components in modern nanophotonics [1–5]. Their ability to create highly localized and intense optical fields has prompted a fundamental reevaluation of light–matter interactions at the nanoscale. The field of plasmonics offers a rich platform for manipulating light at nanometer scales, with applications spanning nanophotonic lasers [6], optical amplifiers [7], metamaterials [8], biochemical sensing [9–11], and nanoantennas [12].

Recent research has increasingly focused on the quantum properties of localized surface plasmons (LSPs) [13–17]. In conventional cavity quantum electrodynamic (CQED) studies, the spontaneous emission of a quantum emitter is enhanced by its placement within an external optical cavity whose spectral and spatial characteristics modify the vacuum fluctuations [18–22].

In plasmonic CQED (PCQED), principles of cavity quantum electrodynamics are implemented to nanoscale plasmonic cavities, in which surface plasmons confine electromagnetic fields to subwavelength volumes with strongly enhanced field intensities. Within these nanostructured electromagnetic environments, the interaction dynamics with an atom- or molecule-like emitter is determined not only by the cavity quality factor, but also by the extremely small effective mode volume [21, 23–25]. Such configurations enable the redistribution of the local density of states (LDOS), leading to either the enhancement or suppression of spontaneous emission on ultrafast time scales via the Purcell effect.

This study explores a fundamentally different regime: the transient free decay of LSPs' excitations in a single metal nanoparticles (NPs). The LSP resonant excitations are modeled as plasmonic quasi-particles (PQPs) that function as the transient emitters of the TM (transverse magnetic) fields, forming a self-created resonant near-field nano-cavity of confined radial fields coupled to the oscillating surface charges. The radially polarized electric fields hold particular significance for light–matter interactions in metal NPs, in the spectral ranges where the real component of the dielectric function is negative. We consider an alteration of a decay process by a structured near-field environment, resulting in the modification of the LDOS available for the plasmonic emitter, which introduces the self-quenching effect due to the intrinsic nonradiative losses in a metal NP.

The quantum modeling developed here is grounded in classical electrodynamics, which provides the eigenfrequencies and damping rates of quasi-normal modes (QNM) of LSPs via dispersion relations for surface-bound TM modes in spherical geometries [26–28]. This classical foundation enabled the construction of a discrete-level quantum many-electron system versus NPs size, allowing for a consistent interpretation of the decay of LSPs excitations in the quasi-particles framework. Overall, the study offers a unified view that bridges classical and quantum perspectives and yields insights into the decay dynamics specific to LSP excitations.

This paper is organized as follows: Sections 2 and 3 revisit crucial aspects of both classical and quantum foundations of localized surface plasmon (LSP) excitations in

metal nanoparticles, necessary for further analysis. Section 4 introduces the fundamentals of spontaneous emission and describes how the Purcell effect results from modified electromagnetic environments. Section 5 presents the central concept of the dual emitter-cavity nature of PQP's decay dynamics. It starts with a classical description of LSP resonances and their relation to a quantum model. It discusses factors influencing the quality factor, the density of optical states associated with confined fields of LSP excitations, and a self-consistent extension of Fermi's Golden Rule for a plasmonic emitter. Finally, Section 6 presents concluding remarks, including a discussion of the physical implications and the specific advantages associated with the investigation of plasmonic nanostructures.

2 Maxwell Picture of Localised Surface Plasmons: Lorenz–Mie Scattering vs. Dispersion Relation

In classical electrodynamics, the response of a spherical nanoparticle (NP) of radius R to an external electromagnetic (EM) wave is described by solving Maxwell's equations with boundary conditions at the NP surface. The EM fields inside and outside the NP are typically expanded using Lorenz–Mie scattering theory as an infinite series of spherical multipole modes with angular momenta $l = 1, 2, 3, \dots$ [29]. The general solution is a sum of transverse magnetic (TM) and transverse electric (TE) modes.

At resonance, the incident EM wave couples efficiently to the curved metal–dielectric interface, generating standing surface waves whose wavelengths scale with R . These waves produce confined radial near-fields and scattered radiation detectable in the far field. LSP resonances are often identified with the maxima in these far-field spectra, which are experimentally observable for NPs of known radii.

However, scattering theory does not explicitly provide the resonance frequencies or damping rates of LSPs. Their dependence on radius, material, and surrounding medium arises from quasinormal modes (QNMs) — complex eigenmode values defined by the dispersion relation (DR) for surface-confined EM waves. These modes are coupled to collective electron oscillations at the metal–dielectric boundary.

2.1 Dispersion Relation for TM Modes

The dispersion relation for QNMs associated with LSPs is derived from the source-free Mie formalism [30], as presented in classical works [26, 29, 31, 32]. Scalar solutions to the Helmholtz equation yield two distinct vectorial modes: TE modes: $E_r = 0$, and TM modes: $E_r \neq 0$, which alone couple to surface charge oscillations.

The complex frequencies of QNMs are roots of the dispersion relation for TM modes with angular momentum l , derived from the continuity of EM field components at the interface $r = R$:

$$\sqrt{\varepsilon_{in}} \xi'_l(k_{out}R) \psi_l(k_{in}R) = \sqrt{\varepsilon_{out}} \xi_l(k_{out}R) \psi'_l(k_{in}R). \quad (1)$$

Here, ε_{in} and $\varepsilon_{out} > 0$ are the dielectric functions of the metal and its environment, respectively. The wave numbers are $k_{in} = \sqrt{\varepsilon_{in}} \omega/c$ and $k_{out} = \sqrt{\varepsilon_{out}} \omega/c$; ψ_l and ξ_l are Riccati–Bessel functions.

Unlike surface plasmon polaritons (SPPs), for which DR yields complex wave vectors for real frequencies, spherical LSP modes require solving for complex eigenfrequencies:

$$\Omega_l(R) = \omega_l(R) - i\Gamma_l(R), \quad (2)$$

where $\omega_l(R)$ is the resonance frequency and $\Gamma_l(R)$ is the total damping rate of LSP oscillations.

The functions $\omega_l(R)$ and $\Gamma_l(R)$ describe discrete standing surface fields, their radial confinement, and far-field radiation. TE modes are not coupled to the interface as they lack solutions at $r = R$, confirming that only TM modes contribute to LSP resonances.

Figure 1a illustrates the dependence $\omega_l(R)$ and $\Gamma_l(R)$ for gold nanospheres for consecutive radii (data from [33]), retardation included).

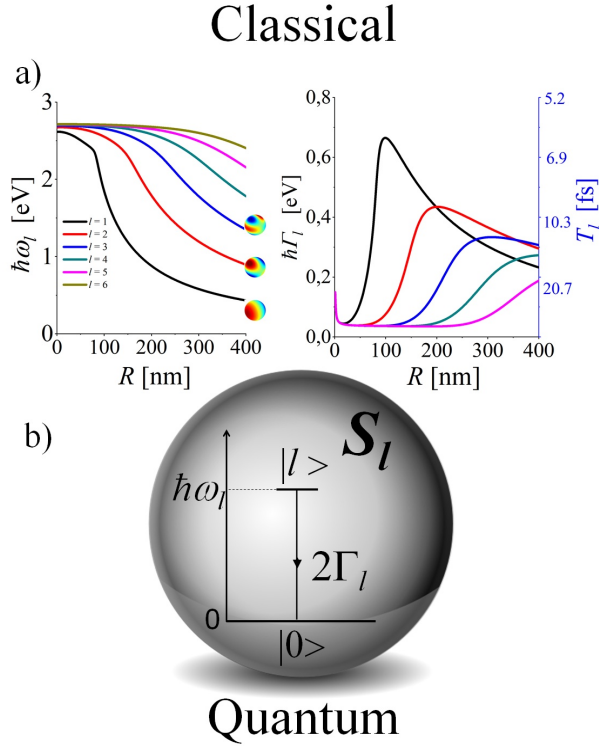


Fig. 1 Classical and quantum representations of LSP dynamics. (a) Resonant frequencies $\hbar\omega_l(R)$ and damping rates $\hbar\Gamma_l(R)$ of QNMs as a function of radius R , including retardation effects [33]. (b) Mapping multipolar modes l to energy levels of a quantum plasmonic quasi-particle (PQP), modeled as independent two-level systems S_l .

Spatial field confinement stems from the negative real part of $\varepsilon_{in}(\omega)$ (anomalous dispersion) in a dielectric medium ($\varepsilon_{out} > 0$), which causes the radial electric field to

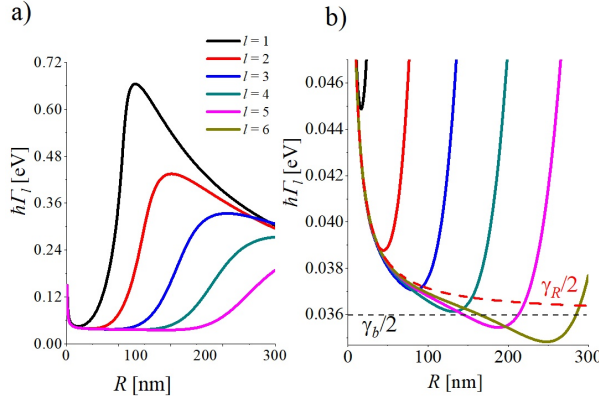


Fig. 2 (a) Total damping rates $\Gamma_l(R)$ (for $l = 1 - 6$) from DR. (b) Close-up view showing that $\Gamma_l(R) \leq \gamma(R)/2$, suggesting non-additivity of radiative and nonradiative terms. Data from [33].

decay evanescently. Outside the NP, radial components fall off as $1/r^2$, and tangential components as $1/r$ [26].

The dispersion relation approach has been extensively studied [34–36] to determine $\omega_l(R)$ and $\Gamma_l(R)$ for a wide range of radii and materials.

2.2 Damping Rates from the Dispersion Relation

The total damping rate $\Gamma_l(R)$ of LSP oscillations (see the example in Fig. 2a)) includes both radiative losses and nonradiative processes resulting from collisional damping. It is often assumed to be additive:

$$\Gamma_l(R) \simeq \Gamma_l^r(R) + \Gamma^{nr}(R), \quad (3)$$

where $\Gamma_l^r(R)$ is the radiative damping rate (from the collisionless model), and $\Gamma^{nr}(R) = \gamma(R)/2$, if assumed to account for electron collisions only, with:

$$\gamma(R) = \gamma_b + \frac{Av_F}{R}. \quad (4)$$

This effective collision rate appears explicitly in ε_{in} , incorporating both bulk ohmic losses γ_b and the size-dependent contribution from surface scattering of electrons, where v_F denotes the Fermi velocity and $C \approx 1$ for noble metals such as Au and Ag (e.g., [34, 36]). The data from [34] (Figure 2) also phenomenologically incorporate the influence of interband transitions on the polarizability. However, the corresponding transition rate is not an explicit parameter in the model of the dielectric function.

In the small size ranges of noble-metal spherical NP's that are experimentally available ($R \lesssim 80\text{nm}$), nonradiative damping with the rate $\Gamma^{nr}(R) = \gamma(R)/2$ dominates (Fig. 2). Dipolar mode ($l = 1$) in this range is weakly radiating, with a small contribution of $\Gamma_l^r(R)$ to $\Gamma_l(R)$ ("low-radiative modes"). Higher-order modes are mostly nonradiative in such a size range ("dark modes").

As R increases, radiative losses grow, eventually dominating total damping ("bright" or radiant modes). Interestingly, numerical results reveal that for some size ranges: (see Fig. 2b):

$$\Gamma_l(R) \leq \Gamma^{nr} = \frac{\gamma(R)}{2}, \quad (5)$$

indicating that a simple additive model is insufficient, as in general: $\Gamma_l(R) \leq \Gamma_l^r(R) + \Gamma^{nr}(R)$. To reconcile this, we define a correction term:

$$\Delta_l(R) := \Gamma_l(R) - (\Gamma_l^r(R) + \Gamma^{nr}) \leq 0, \quad (6)$$

which may stem from a suppression of the nonradiative damping [33, 37]. In particular, Sonnichsen et al. [37] attributed the suppression of nonradiative damping primarily to a reduction in interband transition processes.

However, the arguments based on classical Maxwell electrodynamics do not fully account for the reasons for these reducing corrections to the total damping rate of the radiative modes:

$$\Gamma_l(R) = \Gamma_l^r(R) + \Delta_l(R) + \Gamma^{nr}(R) \leq \Gamma_l^r(R) + \Gamma^{nr}(R). \quad (7)$$

A tentative interpretation of the hypothesis, that introduces the possible co-dependence of the radiative and nonradiative damping channels, and examines the consequences for understanding the intrinsic radiative decay processes of quantum plasmonic emitters, is the subject of the Sections that follow.

3 Foundations for Describing LSPs in Metal Nanoparticles as Quantum Plasmonic Quasi-Particle

The concept of modeling localized surface plasmon (LSP) excitations as quasi-particles arises from their resonant behavior followed by relaxation, observable through the spectral properties of scattered or absorbed light. This approach establishes a bridge between the classical electromagnetic description based on Maxwell's equations and a quantum-mechanical framework where plasmonic excitations are treated as quantized states of a collective many-electron system.

The solutions of the dispersion relation for transverse-magnetic (TM) modes form the classical foundation for the quantum framework. In this view, plasmonic excitations can be conceptualized as discrete, quantized many-electron states with energies $\hbar\omega_l$ (see Figure 1b).

Each multipolar mode l corresponds to a discrete energy level of a quantum plasmonic quasi-particle (PQP), modeled as a set of uncoupled two-level subsystems S_l undergoes transient decay to the ground state $|0\rangle$ after excitation.

Unlike atomic energy levels, the states of a plasmonic quasi-particle $\hbar\omega_l(R)$ originate from the collective oscillations of conduction electrons. The decay of these states includes both population relaxation (energy dissipation) and coherence decay (dephasing). Damping occurs via radiative emission as well as nonradiative mechanisms such

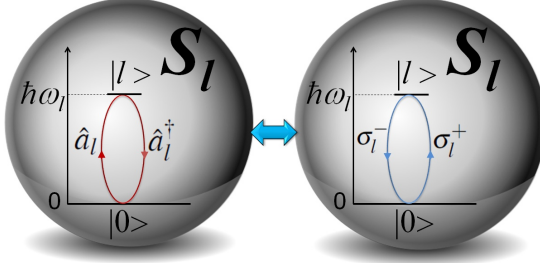


Fig. 3 Conceptual link between the quantum closed cavity-mode model and the plasmonic quasi-particle (PQP) picture. Each TM surface mode of the metal nanoparticle is modeled as a two-level quantum subsystem, with its creation and annihilation operators associated with transitions between ground and excited states.

as ohmic heating caused by electron–electron and electron–surface scattering within the confined NP volume. Nonradiative losses dominate in small nanoparticles, whereas radiative damping becomes the leading process as the particle size increases.

3.1 Closed System. Plasmonic Quasiparticles and Plasmonic Cavities Conceptualized as Equivalent Quantum Systems

In conventional CQED, models such as the Jaynes-Cummings Hamiltonian describe the interaction between a two-level atom and a single quantized mode of an external cavity field [38]. This model assumes a closed system that conserves the number of quanta.

In the specific case of a closed confined subsystem S_l of POP, it forms an integrated quantum system in which quantized TM polarized fields sourced in LSP oscillations and quasi-particle dynamics are intrinsically coupled (see Figure 3). Each surface-cavity mode l is described using an anti-normally ordered Hamiltonian:

Each surface-cavity mode l is described using an anti-normally ordered Hamiltonian:

$$\hat{h}_l^{AN} = \hbar\omega_l \hat{a}_l \hat{a}_l^\dagger, \quad (8)$$

where \hat{a}_l^\dagger and \hat{a}_l are the photon creation and annihilation operators, respectively. These operators are mapped onto the raising and lowering operators $\sigma_l^+ = |l\rangle\langle 0|$ and $\sigma_l^- = |0\rangle\langle l|$, corresponding to transitions between the ground and excited many-electron states of the PQP. The equivalence $\hat{a}_l^\dagger \leftrightarrow \sigma_l^-$ and $\hat{a}_l \leftrightarrow \sigma_l^+$, reflects the process of photon emission corresponding to the transition $|l\rangle \rightarrow |0\rangle$, while excitation corresponds to the reverse process.

The total Hamiltonian of the PQP system, spanning the Hilbert space of the uncoupled two-level modes, is: $\hat{H} = \sum_l \hat{h}_l$, where

$$\hat{h}_l = \hbar\omega_l \sigma_l^+ \sigma_l^- = \hbar\omega_l |l\rangle\langle l|. \quad (9)$$

For each subsystem S_l with the ground state $|0\rangle$ and excited state $|l\rangle$:

$$\hat{h}_l|l\rangle = \hbar\omega_l|l\rangle, \quad \hat{h}_l|0\rangle = 0. \quad (10)$$

Such a self-consistent model provides a compact, physically grounded quantum framework for describing many-electron systems performing coherent collective motion. These systems can be viewed as micro- and macroscopic quantum structures (from tens to hundreds of nanometers in size), sharing characteristics related to the phenomenon of macroscopic quantum coherence demonstrated in superconducting circuits [39, 40] and recently awarded by the Nobel Prize.

3.2 Decay dynamics of plasmonic quasi-particles

In realistic conditions, the plasmonic quasi-particle system $S = \sum_l S_l$ interacts with its environment E , forming an open quantum system. Environmental coupling introduces dissipation and decoherence, leading to energy loss and phase randomization. These effects can be approximately described within the Lindblad master equation formalism under the Markov approximation [41].

For a given subsystem S_l , the evolution of the density matrix $\rho^{S_l}(t)$ is given by:

$$\frac{d\rho^{S_l}}{dt} = -\frac{i}{\hbar}[\hat{h}_l, \rho^{S_l}] + D_l[\rho^{S_l}], \quad (11)$$

where $D_l[\rho^{S_l}]$ is the dissipator:

$$D_l[\rho^{S_l}] = -\frac{1}{2} \sum_{\alpha=r,nr} \left(L_{\alpha,l}^\dagger L_{\alpha,l} \rho^{S_l} + \rho^{S_l} L_{\alpha,l}^\dagger L_{\alpha,l} - 2L_{\alpha,l} \rho^{S_l} L_{\alpha,l}^\dagger \right). \quad (12)$$

The system evolves through two main decay channels: radiative decay, associated with photon emission, modeled by $L_{r,l} = \sqrt{2\Gamma_l^{ref}} \sigma_l^-$ and nonradiative decay, associated with internal losses (ohmic heating, electron-electron or electron-surface scattering), modeled by $L_{nr,l} = \sqrt{2\Gamma^{nr}} \sigma_l^-$. The radius dependence of the rates $\Gamma_l^{ref}(R)$ and $\Gamma^{nr}(R)$ follows from the classical modeling.

Solving the Lindblad equation for POP [17, 42] yields exponentially decaying populations and coherences:

$$\rho_{ll}(t) = \rho_{ll}(t_0) \exp(-2\Gamma_l t), \quad (13)$$

$$\rho_{00}(t) = \rho_{ll}(t_0)(1 - \exp(-2\Gamma_l t)), \quad (14)$$

$$\rho_{l0}(t) = \rho_{0l}(t_0) \exp((i\omega_l - \Gamma_l)t) = \rho_{0l}(t), \quad (15)$$

where $\Gamma_l(R)$ are derived within the classical model (Eq. (7)).

The population which are proportional to $\rho_{ll}(t)$ of the excited state decays as $e^{-2\Gamma_l t}$: while the oscillations of coherences (of the off-diagonal terms $\rho_{l0}(t), \rho_{0l}(t)$) decay twice as slowly, with a rate Γ_l . This behavior aligns with the general expectation

that coherence decays more slowly than population, primarily due to its reliance on phase randomisation. In metal nanoparticles, the total rate Γ_l , along with the radiative and non-radiative contributions, varies with nanoparticle size and is ultimately determined by the intrinsic electrodynamic properties of the metal nanoparticle.

4 Concept of Spontaneous Emission

4.1 Fundamental Concepts of Spontaneous Emission

Spontaneous emission in a free space, observed in quantum emitters like atoms or molecules, occurs due to vacuum electromagnetic fluctuations. These fluctuations enable transitions between energy states, with the emission rate determined by the spectral density of vacuum modes evaluated at the emitter's transition frequency.

In a two-level atom, the spontaneous emission rate in vacuum is given by the Weisskopf–Wigner formula:

$$\Gamma_{21} = \frac{\omega_{21}^3 d_{12}^2}{3\pi\epsilon_0\hbar c^3}, \quad (16)$$

where ω_{21} is the transition frequency and d_{12} is the dipole matrix element. This expression is sometimes analogously applied to describe the radiative damping of dipolar LSP modes (e.g. [43]).

When the emitter is placed in an inhomogeneous medium, such as an optical cavity, the spontaneous emission rate is modified by the available EM states of the surrounding environment, altering the vacuum field mode structure and the local density of states. As a result, the emission rate can be enhanced or suppressed compared to that in free space (e.g., [3, 44]. This fundamental sensitivity of spontaneous emission to the electromagnetic environment forms the basis of CQED (e.g., [45–49]) and underpins emission control in structured photonic media.

4.2 Cavity LDOS and the Purcell Effect

Cavity quantum electrodynamics (CQED) and its plasmonic counterpart (PQED) investigate how optical and plasmonic cavities affect spontaneous emission via the Purcell effect, which quantifies enhancement (or suppression) of emission due to increased LDOS near the emitter's resonance [18, 19, 21].

Unlike free space, where EM modes form a continuum, a cavity supports discrete modes of frequency ω_l and finite linewidth $\Delta\omega_l$ of these modes. The quality factor of a cavity mode $Q = \omega_l/\Delta\omega_l$, states how sharply localized the mode is in frequency. High- Q cavities concentrate the photonic density of states near the cavity's resonance frequency ω_{cav} .

The Purcell factor F_P , expressing the enhancement of spontaneous emission relative to free space, is commonly expressed as:

$$F_P = \frac{3}{4\pi^2} \left(\frac{\lambda}{n} \right)^3 \frac{Q}{V_{eff}}, \quad (17)$$

where λ is the emission wavelength, n is the refractive index of the medium and V_{eff} is the effective mode volume of the cavity.

The Purcell effect is directly related to the density of photonic states at the emitter's frequency ω_0 . Its derivation can be based on the arguments derived from Fermi's golden rule, which states that the transition rate for the emitter is proportional to the LDOS at the emitter's resonance.

For a resonant cavity, the LDOS can be approximated by a Lorentzian distribution:

$$\rho_{cav}(\omega) = \frac{1}{V_{eff}} \cdot \frac{\Delta\omega_{cav}}{(\Delta\omega_{cav})^2 + (\omega - \omega_{cav})^2}. \quad (18)$$

At resonance ($\omega_{cav} = \omega_0$), this simplifies to:

$$\rho_c(\omega_0) = \frac{Q}{\omega_0 V_{eff}}. \quad (19)$$

Thus, the Purcell factor relates to the ratio of cavity to free-space LDOS:

$$F_P = \frac{\Gamma_c}{\Gamma_f} = M \cdot \frac{\rho_c(\omega_0)}{\rho_f(\omega_0)} = \frac{1}{V_{eff}} \cdot \frac{Q}{\omega_0} \cdot \frac{\pi^2 c^3}{\omega_0^2}, \quad (20)$$

where M accounts for mode overlap. This expression highlights that maximizing the emission enhancement requires both a high Q and a small mode volume V_{eff} .

For the conventional emitters in a plasmonic cavity, strong field confinement leads to very small V_{eff} , enabling high Purcell enhancement despite low Q . Plasmonic cavities of different geometries (e.g., bowtie, gap antenna) are essential tools in nanophotonics for squeezing light down to the nanoscale to unlock powerful light-matter interactions. However, in proximity to metallic surfaces, nonradiative decay processes become predominant, leading to quenching of the emission and a concomitant decrease in the lifetime of the emitter (e.g. [20, 21, 50–56]).

5 The Dual Functionality of Plasmonic Quasi-Particles

In conventional cavity quantum electrodynamics (CQED) and plasmonic CQED (PCQED), spontaneous emission is typically studied in systems where an external cavity modifies the emission rate of an adjacent atom-like emitter. The cavity alters the local density of optical states (LDOS) available to the emitter, enhancing or suppressing spontaneous emission via the Purcell effect. In such systems, the emitter and the cavity are separate entities, and the cavity's spectral properties remain unaffected by the emitter.

In contrast, the excited plasmonic nanoparticle plays a dual role, acting as a source of plasmonic cavity and the TM emitter embedded in a cavity of confined longitudinal near-field modes. The same physical structure allows the collective surface charge oscillations for a certain time in the femtosecond range (Fig. 1a)) after the LSP excitation. These oscillations are a source of the locally confined longitudinal fields, which leak from the surface, and decay as $1/r^2$ (see Section 2). The longitudinal evanescent field modes coupled to the oscillating surface charges do not radiate energy away. Instead, they act as a storage of reactive energy, while the tangential field components decay as $1/r$, carrying part of the energy to the far field region.

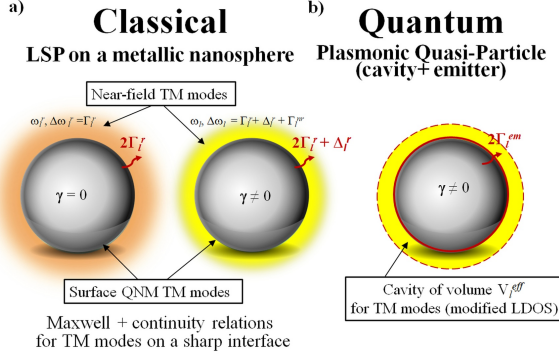


Fig. 4 a) Classical picture of a metal nanoparticle supporting LSP resonant oscillations embedded in the near-field region, which contains the nonzero component of the electric field E_l^r coupled to surface charge oscillations. The spectral characteristics of the interface and the near field are identical at and near resonance, but are modified in the collisionless electron regime. (b) Corresponding quantum picture: the near-field region is represented by the effective volume V_l^{eff} , forming a cavity with a modified LDOS. Plasmon energy is emitted into this self-generated cavity, which is inherently coupled to the emitter.

Accordingly, the interface and the adjacent near-field region can be conceptualized as the cavity of the effective volume V_l^{eff} (Fig. 4a)), with dimensions that scale with the size of the particle. Both the emitter and the cavity share the same spectral properties and are dynamically coupled. This coupling is a defining feature of PQPs that has no counterpart in traditional atomic systems, leading to spontaneous emission dynamics fundamentally distinct from those in conventional atom-like or atom–cavity systems, where such mutual dependence does not exist.

Bridging the classical and quantum pictures, we adopt a self-consistent model where:

- The plasmonic emitter is modeled as a sum of two-level quantum systems with excited state $|l\rangle$, ground state $|0\rangle$, and transition energy $\hbar\omega_l$. The decay of the excited state to the ground state takes place at the rate Γ_l^{ref} , which is the damping rate resulting from photon emission in the presence of electron collisions.
- The plasmonic cavity is characterized by the effective volume V_l^{eff} defining the evanescent near-field region, resonance frequency ω_l^c , and total spectral width Γ_l^c of the evanescent fields, resulting from both radiative and nonradiative contributions.
- The emitter and the cavity share identical spectral parameters, such that $\omega_l^c = \omega_l$ and $\Gamma_l^c = \Gamma_l = \Gamma_l^{ref} + \Gamma^{nr}$.

Therefore, nonradiative losses, such as electron scattering, affect not only the emitter's linewidth but also the photonic environment itself, by broadening the local density of optical states (LDOS) available for the emitter. This behavior fundamentally differs from the conventional Purcell effect, in which the cavity spectrum remains unaffected by the emitter.

In summary, the effective volume V_l^{eff} provides a geometric and physical link between the classical near-field confinement and the quantum LDOS into which emission occurs (Fig. 4). This bridge enables a consistent formulation of spontaneous emission rates for plasmonic quasi-particles based on Fermi's golden rule, incorporating both the emitter and the structured EM environment as a single, self-consistent system.

5.1 Quality Factor of Plasmonic Cavity

The quality factor of the plasmonic cavity $Q_l(R)$, [23, 36, 47, 57] defined as the number of oscillations required for the energy of a freely oscillating system to fall off to $e^{-2\pi}$ of its original energy, is a function of the radius R of MNP:

$$Q_l(R) = \hbar\omega_l^c(R)/\Delta E_l(R) = \omega_l^c(R)/\Gamma_l^c(R), \quad (21)$$

where ω_l^c is the resonance frequency of the mode and $\Delta\omega_l^c = \Gamma_l^c$ is the total linewidth of the cavity mode due to both radiative and nonradiative processes.

As the surface TM fields and the concentrated fields around the plasmonic emitter possess the same spectral parameters, solutions of the dispersion relation (Eq. (1)) yield:

$$\Gamma_l(R) = \Gamma_l^c(R), \quad (22)$$

where Γ_l^c is composed of the radiative Γ_l^{ref} and nonradiative Γ^{nr} contributions (Eq (7)).

The quality factor thus encapsulates both the intrinsic resonant confinement of the EM field (via ω_l) and the loss mechanisms that limit the ability of the cavity to store the total energy of LSP excitation. It plays a central role in determining LDOS, which in turn controls the emission dynamics of the plasmonic emitter.

5.2 Density of States of Plasmonic Cavity Created by Plasmonic Quasiparticle

The LDOS of plasmonic cavities (including those created by a PQP emitter) depends on the spectral and spatial characteristics of the LSP; therefore, it differs from the LDOS of freely decaying atomic systems in which the photonic environment is unstructured, but also from the LDOS of optical cavities (Eq. (18)). The spectral identity between emitter and cavity makes the plasmonic emitter fundamentally different from standard emitters studied in CQED and PCQED.

The LDOS quantifies the number of electromagnetic modes available for photon emission per unit volume and frequency. Therefore, in the case of a single-mode plasmonic cavity characterised by an effective volume V_l^{eff} and resonance frequency ω_l , the LDOS (Eqs. (18)) of PQP's created cavity can be expressed as:

$$\rho^p(\omega_l) = \frac{1}{V_l^{eff}\Delta\omega_l^c} = \frac{Q_l}{\omega_l V_l^{eff}}, \quad (23)$$

where $\Delta\omega_l^c$ is the full width at half maximum (FWHM) of the cavity resonance, linked to the total loss rate $\Delta\omega_l^c = \Gamma_l^c = \Gamma_l(R)$ (Eqs. (7), (22) of the mode and Q_l is the quality factor.

Consequently, the density of states ρ^p that is available for the emitter is affected by intrinsic material losses, such as ohmic attenuation and surface scattering (Eq. 4).

Conversely, traditional CQED and PCQED systems use an external, independent resonators. Within the PQP framework, the correspondence between the emitter and cavity parameters necessitates a novel, self-consistent formulation of the spontaneous emission decay from the confined plasmonic systems.

5.3 Extension of Fermi's Golden Rule to PQP Systems

Fermi's Golden Rule (FGR) provides a foundational quantum framework for calculating transition rates in systems weakly coupled to a continuum of final states. For spontaneous emission, it is typically given by:

$$\Gamma_{if} = \frac{2\pi}{\hbar} |\langle f | \hat{H}' | i \rangle|^2 \rho(E_f), \quad (24)$$

where $|i\rangle$ and $|f\rangle$ are the initial and final quantum states, \hat{H}' is the interaction Hamiltonian, and $\rho(E_f)$ is the density of final states at energy E_f . This expression assumes an external, EM environment independent of the emitter.

In contrast, a plasmonic quasi-particle (PQP) forms a self-consistent system where both the emitter and the cavity originate from the same physical structure and share the same spectral parameters. The emission occurs into a structured, near-field environment that is dynamically coupled to the emitter.

To account for this, we extend FGR by incorporating the cavity LDOS (Eq. 23)):

$$\Gamma_l^p = \frac{2\pi V_l}{\hbar} |\langle l | \hat{V} | 0 \rangle|^2 \rho^p(\hbar\omega_l) = \frac{2\pi V_l}{\hbar^2} \frac{|\langle l | \hat{V} | 0 \rangle|^2}{V_l^{eff} \Gamma_l^c}, \quad (25)$$

where: $\Gamma_l^p = 2\Gamma_l^{ref}$ is the spontaneous emission rate, and $\Gamma_l^c = \Gamma_l^{ref} + \Gamma^{nr}$ is the total linewidth of the PQP cavity. The matrix element $|\langle l | \hat{V} | 0 \rangle|^2$ is renormalized by a mode confinement factor $\beta_l = V_l/V_l^{eff}$.

In the collisionless limit ($\Gamma^{nr} = 0$), Eq. (25) simplifies to:

$$2\Gamma_l^r = \frac{2\pi V_l}{\hbar^2} |\langle l | \hat{V} | 0 \rangle|^2 \frac{1}{V_l^{eff} \Gamma_l^c}, \quad (26)$$

which allows us to express the interaction strength as:

$$\frac{2\pi}{\hbar^2} |\langle l | \hat{V} | 0 \rangle|^2 = \frac{2\Gamma_l^r \Gamma_l^{cr} V_l^{eff}}{V_l}. \quad (27)$$

Substituting this into Eq. (25) for the general lossy case gives:

$$\Gamma_l^p = 2\Gamma_l^{ref} = \frac{2\Gamma_l^r \Gamma_l^{cr}}{\Gamma_l^c} = \frac{2(\Gamma_l^r)^2}{\Gamma_l^{ref} + \Gamma^{nr}}, \quad (28)$$

which yields the self-consistent radiative emission rate:

$$\Gamma_l^{ref} = \frac{1}{2} \left(\sqrt{4(\Gamma_l^r)^2 + (\Gamma^{nr})^2} - \Gamma^{nr} \right) \leq \Gamma_l^r. \quad (29)$$

This expression reveals a self-quenching effect, in which a nonradiative decay channel attenuates radiative emission as a consequence of the dynamic coupling between the emitter and the cavity. This mechanism is fundamentally different from classical Purcell suppression, since it arises from the dissipative characteristics of the emitter's immediate self-created EM environment.

Nonetheless, it can be viewed as analogous to fluorescence quenching in conventional PQED architectures (Section 4.2), which occurs when an atomic or molecular emitter is placed in close proximity to a plasmonic nanoparticle [20, 21, 50–56].

In limiting cases:

$$\begin{aligned} \text{If } \Gamma^{nr} \ll \Gamma_l^r, \text{ then } \Gamma_l^{ref} &\approx \Gamma_l^r; \\ \text{If } \Gamma^{nr} \gg \Gamma_l^r, \text{ then } \Gamma_l^{ref} &\ll \Gamma_l^r. \end{aligned}$$

In general, the total damping rate of the PQP becomes:

$$\Gamma_l(R) = \Gamma_l^{ref}(R) + \Gamma^{nr}(R) \leq \Gamma_l^r(R) + \Gamma^{nr}(R). \quad (30)$$

The structure of Eq. 29 explicitly illustrates the non-additive character of the decay channels. The intrinsic nonradiative losses in metal NPs do not merely contribute linearly to the LSP damping. Instead, they can dynamically suppress the total decay rate within certain regions of the parameter space.

The reduction of the total damping rate $\Gamma_l(R)$ is consistent with our predictions based on classical electrodynamics (Eq. (7)). The quenching effect manifests in low-radiative modes within the size and multipolarity ranges for which $0 < \Gamma_l^r(R) \leq \Gamma_l^{nr}(R)$ (Fig. 2b).

While the self-quenching effect described by Eq. 29 is consistent with the qualitative trends observed in our classical results (Section 2), a quantitative validation requires separating the radiative component $\Gamma_l^r(R)$ from the total damping rate $\Gamma_l(R)$. This decomposition was not part of our previous classical analysis, which focused on total damping. Additionally, explicit parametrization of interband transitions, which dominate $\Gamma_l^{nr}(R)$ at small radii, is necessary but currently incomplete. A detailed classical study addressing both aspects is underway and will be reported separately.

5.4 Correspondence to the experimental observations

Experimental investigations of localized surface plasmon (LSP) damping in noble-metal nanoparticles conventionally represent the total damping rate as the linear superposition of independent radiative and nonradiative contributions. Nonetheless, several studies (e.g. [33, 37, 43, 58]) have reported anomalous behavior that departs from the standard assumptions in specific systems and experimental conditions.

In [37], the authors study plasmon damping rates in single gold nanoparticles using dark-field spectroscopy to record light-scattering spectra as a function of particle

size and shape. The study demonstrates that in the spherical NPs, the homogeneous broadening (dephasing rate) of the plasmon resonance increases with particle size due to enhanced radiation damping, as expected. In contrast, in nanorods, the dephasing rate of a low radiative dipole LSP resonance drastically decreases with increasing length. The authors attribute this unexpected effect to suppressed interband damping, which contributes to nonradiative damping. Their supporting quasistatic calculations neglect radiation damping.

The results for the dipole mode of nanospheres remain in accordance with our expectations in the studied range of sizes $2R = 20, \dots, 150$ nm, as illustrated in Fig. 2b)) (black line).

Nanorods, in contrast, offer more favorable conditions for observing the self-quenching effect. The long-axis mode behaves nearly as an ideal dipolar emitter with low (suppressed) radiative losses, even for larger sizes. Therefore, the condition $\Gamma^{nr} > \Gamma_l^r$ is fulfilled. According to Eq. 29), in such a range of parameters, one can expect suppression of the radiative damping with the increasing NP size, as illustrated for higher-order modes in spherical NPs (Fig. 2b)).

More direct evidence of the coupling between radiative and nonradiative channels was provided by recent TR-PEEM (Time-Resolved PhotoEmission Electron Microscopy) experiments on gold nanorods [59]. The authors measured lifetimes of bright (superradiant) and dark (subradiant) modes as a function of nanorod length. Surprisingly, bright modes were found to have lifetimes equal to or longer than those of subradiant modes, contradicting the expectation that radiative losses shorten the lifetimes of bright modes: $\Gamma^{super}(\Gamma^r, \Gamma^{nr}) \leq \Gamma^{subr}(\Gamma^{nr})$, despite the presence of radiative damping in the superradiant case. This confirms the co-dependence of decay channels Eq. 29).

This behavior directly supports our prediction (Eq. 29). It demonstrates the non-additivity of decay channels. The presence of inherent nonradiative losses in metal NPs does not simply add to the LSP damping. Instead, it can dynamically suppress the total decay rates in some parameter ranges.

6 Conclusions

This work presents a unified, quantum-informed framework in which decaying localized surface plasmon (LSP) excitations are conceptualized as plasmonic quasi-particles - quantized, coherent many-electron emitters that radiate energy into their own structured near-field TM-polarized electromagnetic environment. The excited plasmonic emitter and its self-generated EM environment form the cavity of TM confined field modes, sharing the same transient dynamics as the source fields of LSP. Therefore, both the decay rates of surface TM-polarized fields and cavity fields are composed of radiative and nonradiative contributions.

An intrinsic suppression of the total damping rate of radiative modes due to the self-quenching effect is predicted. This effect does not arise from an externally altered EM environment as in the traditional Purcell effect. Rather, it occurs due to the loss of part of the excitation energy via collisional, ohmic losses in a metal NP, resulting in heat generation. Consequently, the emission characteristics of the plasmonic system

are modified self-consistently, as the effective LDOS, dependent on the quality factor of the self-created plasmonic cavity, is influenced by the nonradiative losses process, which introduces a co-dependence of radiative and non-radiative decay channels.

Thus, the conventional view of LSP decay as a sum of independent radiative and nonradiative channels is no longer sufficient in general. Instead, radiative emission is inherently reduced due to the self-quenching effect.

These result aligns with our description of the transient LSP decay in classical frames of Maxwell electrodynamics and help explain experimental observations of anomalously long lifetimes in nanorods [37, 59]. Classically derived cavity parameters, obtained from the dispersion relation of quasi-normal transverse-magnetic (TM) multipolar modes (retardation effects included), form the foundation of our model. Their reinterpretation within the self-consistent quantum framework offers a physically transparent bridge between Maxwell and quantum descriptions of LSP dynamics.

Beyond its implications for emission control, the model highlights the bosonic nature of PQPs: coherent excitations of many-electron systems that behave collectively as quantized states. These systems can be viewed as micro- and macroscopic quantum structures, sharing characteristics related to the phenomenon of macroscopic quantum coherence. These localized surface-bound bosonic modes form without nonlinear thresholds and can exist at room temperature. Unlike traditional Bose–Einstein condensates (BECs), which require ultralow temperatures and massive particles, PQPs provide a platform for studying room-temperature bosonic phenomena in three-dimensional systems. This insight aligns with recent demonstrations of polariton and quasiparticle condensation under ambient conditions [60, 61], further validating the relevance of the PQP model.

The self-consistent, quantum-local framework for a deeper understanding of the decay process in coherent many-electron micro- and macro-systems presented here can possibly serve in the development of decay engineering, controlled light–matter interactions, and the development of future quantum technologies based on highly dissipative yet coherent plasmonic systems.

7 Funding Declarations

This research was funded in whole or in part by the National Science Centre, Poland, grant 2021/41/B/ST3/00069. For the purpose of Open Access, the authors have applied a CC-BY public copyright license to any Author Accepted Manuscript (AAM) version arising from this submission.

8 Availability of data and materials

All data supporting the findings of this study are either presented within the manuscript or based on previously published results, as referenced in [33]: K. Kolwas and A. Derkachova, "Damping rates of surface plasmons for particles of size from nano- to micrometers; reduction of the nonradiative decay," *JQSRT*, 114 (2013), pp. 45–55. No new datasets were generated or analyzed specifically for this work.

References

- [1] Barnes, W.L., Dereux, A., Ebbesen, T.W.: Surface plasmon subwavelength optics. *Nature* **424**(6950), 824–830 (2003)
- [2] Schuller, J.A., Barnard, E.S., Cai, W., Jun, Y.C., White, J.S., Brongersma, M.L.: Plasmonics for extreme light concentration and manipulation. *Nature materials* **9**(3), 193–204 (2010)
- [3] Novotny, L., Hecht, B.: Principles of Nano-optics. Cambridge University Press, ??? (2012)
- [4] Alekseeva, S., Nedrygailov, I.I., Langhammer, C.: Single particle plasmonics for materials science and single particle catalysis. *ACS Photonics* **6**(6), 1319–1330 (2019)
- [5] Nam, J.-M., Liz-Marzán, L., Halas, N.: Chemical nanoplasmonics: emerging interdisciplinary research field at crossroads between nanoscale chemistry and plasmonics. *ACS Publications* (2019)
- [6] Gaio, M., Saxena, D., Bertolotti, J., Pisignano, D., Camposeo, A., Sapienza, R.: A nanophotonic laser on a graph. *Nature communications* **10**(1), 226 (2019)
- [7] Qin, W., Kockum, A.F., Muñoz, C.S., Miranowicz, A., Nori, F.: Quantum amplification and simulation of strong and ultrastrong coupling of light and matter. *Physics Reports*, or arXiv preprint arXiv:2401.04949 **69**, 1–59 (2024)
- [8] Cai, W., Shalaev, V.: Optical Metamaterials. Springer, ??? (2010)
- [9] Aslan, K., Lakowicz, J.R., Geddes, C.D.: Plasmon light scattering in biology and medicine: new sensing approaches, visions and perspectives. *Curr. Opin. Chem. Biol.* **9**(5), 538–544 (2005)
- [10] Jain, P.K., Huang, X., El-Sayed, I.H., El-Sayed, M.A.: Review of some interesting surface plasmon resonance-enhanced properties of noble metal nanoparticles and their applications to biosystems. *Plasmonics* **2**(3), 107–118 (2007)
- [11] Shalabney, A., Abdulhalim, I.: Sensitivity-enhancement methods for surface plasmon sensors. *Laser & Photonics Reviews* **5**(4), 571–606 (2011)
- [12] Monticone, F., Argyropoulos, C., Alu, A.: Optical antennas: controlling electromagnetic scattering, radiation, and emission at the nanoscale. *IEEE Antennas and Propagation Magazine* **59**(6), 43–61 (2017)
- [13] Jacob, Z., Shalaev, V.M.: Plasmonics goes quantum. *Science* **334**(6055), 463–464 (2011)
- [14] Van Vlack, C., Kristensen, P.T., Hughes, S.: Spontaneous emission spectra and

quantum light-matter interactions from a strongly coupled quantum dot metal-nanoparticle system. *Phys. Rev. B* **85**(7), 075303 (2012)

[15] Scholl, J.A., Koh, A.L., Dionne, J.A.: Quantum plasmon resonances of individual metallic nanoparticles. *Nature* **483**(7390), 421–427 (2012)

[16] Bozhevolnyi, S.I., Mortensen, N.A.: Plasmonics for emerging quantum technologies. *Nanophotonics* **6**(5), 1185–1188 (2017)

[17] Kolwas, K.: Decay dynamics of localized surface plasmons: Damping of coherences and populations of the oscillatory plasmon modes. *Plasmonics* **14**(6), 1629–1637 (2019)

[18] Haroche, S., Kleppner, D.: Cavity quantum electrodynamics. *Physics Today* **42**, 24–30 (1989) <https://doi.org/10.1063/1.881201>

[19] Walther, H., Varcoe, B.T., Englert, B.-G., Becker, T.: Cavity quantum electrodynamics. *Reports on Progress in Physics* **69**(5), 1325 (2006)

[20] Guzatov, D.V., Vaschenko, S.V., Stankevich, V.V., Lunovich, A.Y., Glukhov, Y.F., Gaponenko, S.V.: Plasmonic enhancement of molecular fluorescence near silver nanoparticles: theory, modeling, and experiment. *The Journal of Physical Chemistry C* **116**(19), 10723–10733 (2012)

[21] Hugall, J.T., Singh, A., Hulst, N.F.V.: Plasmonic cavity coupling. *ACS Photonics* **5**, 43–53 (2018) <https://doi.org/10.1021/acsphotonics.7b01139>

[22] Franke, S., Hughes, S., Dezfooli, M.K., Kristensen, P.T., Busch, K., Knorr, A., Richter, M.: Quantization of quasinormal modes for open cavities and plasmonic cavity quantum electrodynamics. *Physical review letters* **122**(21), 213901 (2019)

[23] Kristensen, P.T., Hughes, S.: Modes and mode volumes of leaky optical cavities and plasmonic nanoresonators. *ACS Photonics* **1**, 2–10 (2014) <https://doi.org/10.1021/ph400114e> . Review

[24] Ginzburg, P.: Cavity quantum electrodynamics in application to plasmonics and metamaterials. *Reviews in Physics* **1**, 120–139 (2016)

[25] Wei, H., Yan, X., Niu, Y., Li, Q., Jia, Z., Xu, H.: Plasmon–Exciton Interactions: Spontaneous Emission and Strong Coupling. John Wiley and Sons Inc (2021). <https://doi.org/10.1002/adfm.202100889>

[26] Fuchs, R., Halevi, P.: Spatial Dispersion in Solids and Plasmas. Amsterdam ; New York : North-Holland, ??? (1992)

[27] Kolwas, K., Demianiuk, S., Kolwas, M.: Optical excitation of radius-dependent plasmon resonances in large metal clusters. *Journal of Physics B: Atomic, Molecular and Optical Physics* **29**(20), 4761 (1996)

[28] Kolwas, K., Derkachova, A., Demianiuk, S.: The smallest free-electron sphere sustaining multipolar surface plasmon oscillation. *Comput. Mat. Sci.* **35**(3), 337–341 (2006)

[29] Born, M., Wolf, E.: *Principles of Optics: Electromagnetic Theory of Propagation, Interference and Diffraction of Light*. Cambridge university press, ??? (1999)

[30] Mie, G.: Beiträge zur optik trüber medien, speziell kolloidaler metallösungen. *Ann. Phys.* **25**(3), 377–445 (1908)

[31] Stratton, J.A.: *Electromagnetic Theory*. John Wiley & Sons, ??? (2007)

[32] Ruppin, R.: *Electromagnetic Surface Modes* vol. 9, p. 349. Wiley, Chichester, ??? (1982)

[33] Kolwas, K., Derkachova, A.: Damping rates of surface plasmons for particles of size from nano-to micrometers; reduction of the nonradiative decay. *JQSRT* **114**, 45–55 (2013)

[34] Derkachova, A., Kolwas, K., Demchenko, I.: Dielectric function for gold in plasmonics applications: Size dependence of plasmon resonance frequencies and damping rates for nanospheres. *Plasmonics* **11**(3), 941–951 (2016)

[35] Kolwas, K., Derkachova, A.: Modification of solar energy harvesting in photovoltaic materials by plasmonic nanospheres: New absorption bands in perovskite composite film. *J. Phys. Chem. C* **121**(8), 4524–4539 (2017)

[36] Kolwas, K., Derkachova, A.: Impact of the interband transitions in gold and silver on the dynamics of propagating and localized surface plasmons. *Nanomaterials* **10**, 1411 (2020) <https://doi.org/10.3390/NANO10071411>

[37] Sonnichsen, C., Franzl, T., Wilk, T., Plessen, G., Feldmann, J., Wilson, O., Mulvaney, P.: Drastic reduction of plasmon damping in gold nanorods. *Phys. Rev. Lett.* **88**(7), 077402–077402 (2002)

[38] Jaynes, E.T., Cummings, F.W.: Comparison of quantum and semiclassical radiation theories with application to the beam maser. *Proceedings of the IEEE* **51**(1), 89–109 (1963)

[39] Devoret, M.H., Martinis, J.M., Clarke, J.: Measurements of macroscopic quantum tunneling out of the zero-voltage state of a current-biased josephson junction. *Physical review letters* **55**(18), 1908 (1985)

[40] Martinis, J.M., Devoret, M.H., Clarke, J.: Energy-level quantization in the zero-voltage state of a current-biased josephson junction. *Physical review letters* **55**(15), 1543 (1985)

[41] Breuer, H.P., Petruccione, F., *et al.*: *The Theory of Open Quantum Systems*.

Oxford University Press on Demand, ??? (2002)

- [42] Kolwas, K.: Optimization of coherent dynamics of localized surface plasmons in gold and silver nanospheres; large size effects. *Materials* **16**(5), 1801 (2023)
- [43] Moustafa, S., Zayed, M.K., Ahmed, M., Fares, H.: Bandwidth of quantized surface plasmons: competition between radiative and nonradiative damping effects. *Physical Chemistry Chemical Physics* **26**, 1994–2006 (2023) <https://doi.org/10.1039/d3cp04564a>
- [44] Martín-Cano, D., Huidobro, P.A., Moreno, E., García-Vidal, F.: Quantum plasmonics. In: *Handbook of Surface Science* vol. 4, pp. 349–379. Elsevier, ??? (2014)
- [45] Maier, S.A.: Effective mode volume of nanoscale plasmon cavities. *Optical and Quantum Electronics* **38**, 257–267 (2006)
- [46] Kristensen, P.T., Van Vlack, C., Hughes, S.: Generalized effective mode volume for<? a3b2 show [pmg: line-break justify=" yes"/]?> leaky optical cavities. *Optics letters* **37**(10), 1649–1651 (2012)
- [47] Derom, S., Vincent, R., Bouhelier, A., Francs, G.C.: Resonance quality, radiative/ohmic losses and modal volume of mie plasmons. *EPL* **98**(4), 47008 (2012)
- [48] Sauvan, C., Hugonin, J.-P., Maksymov, I., Lalanne, P.: Theory of the spontaneous optical emission of nanosize photonic and plasmon resonators. *Physical Review Letters* **110**(23), 237401 (2013)
- [49] Pelton, M.: Modified spontaneous emission in nanophotonic structures. *Nature Publishing Group* (2015). <https://doi.org/10.1038/nphoton.2015.103>
- [50] Lakowicz, J.R.: Radiative decay engineering 5: metal-enhanced fluorescence and plasmon emission. *Analytical biochemistry* **337**(2), 171–194 (2005)
- [51] Anger, P., Bharadwaj, P., Novotny, L.: Enhancement and quenching of single-molecule fluorescence. *Physical review letters* **96**(11), 113002 (2006)
- [52] Bharadwaj, P., Anger, P., Novotny, L.: Nanoplasmonic enhancement of single-molecule fluorescence. *Nanotechnology* **18**(4), 044017 (2006)
- [53] Olejnik, M., Bujak, L., Mackowski, S.: Plasmonic molecular nanohybrids—spectral dependence of fluorescence quenching. *International Journal of Molecular Sciences* **13**(1), 1018–1028 (2012)
- [54] Rasskazov, I.L., Wang, L., Murphy, C.J., Bhargava, R., Carney, P.S.: Plasmon-enhanced upconversion: engineering enhancement and quenching at nano and macro scales. *Optical Materials Express* **8**(12), 3787–3804 (2018)

- [55] Kongsuwan, N., Demetriadou, A., Chikkaraddy, R., Benz, F., Turek, V.A., Keyser, U.F., Baumberg, J.J., Hess, O.: Suppressed quenching and strong-coupling of purcell-enhanced single-molecule emission in plasmonic nanocavities. *Acs Photonics* **5**(1), 186–191 (2018)
- [56] Hildebrandt, N., Lim, M., Kim, N., Choi, D.Y., Nam, J.-M.: Plasmonic quenching and enhancement: metal–quantum dot nanohybrids for fluorescence biosensing. *Chemical Communications* **59**(17), 2352–2380 (2023)
- [57] Stockman, M.I., Kneipp, K., Bozhevolnyi, S.I., Saha, S., Dutta, A., Ndukaife, J., Kinsey, N., Reddy, H., Guler, U., Shalaev, V.M., *et al.*: Roadmap on plasmonics. *Journal of Optics* **20**(4), 043001 (2018)
- [58] Ginzburg, P., Zayats, A.V.: Non-exponential decay of dark localized surface plasmons. *Optics Express* **20**(6), 6720–6727 (2012)
- [59] Qin, Y., Xu, Y., Ji, B., Song, X., Lin, J.: Coaction effect of radiative and non-radiative damping on the lifetime of localized surface plasmon modes in individual gold nanorods. *The journal of chemical physics* **158**(10) (2023)
- [60] Lagoudakis, K.G., Pietka, B., Wouters, M., André, R., Deveaud-Plédran, B.: Coherent oscillations in an exciton-polariton josephson junction. *Physical review letters* **105**(12), 120403 (2010)
- [61] Kędziora, M., Opala, A., Mastria, R., De Marco, L., Król, M., Łempicka-Mirek, K., Tyszka, K., Ekielski, M., Guziewicz, M., Bogdanowicz, K., *et al.*: Pre-designed perovskite crystal waveguides for room-temperature exciton–polariton condensation and edge lasing. *Nature Materials*, 1–8 (2024)